The Role of Magnetic Field in State Transitions of BHXBs

Ding-Xiong Wang

Huazhong University of Science & Technology

Outline of this talk

The role of magnetic field is discussed in the following aspects:

1. **Jet production in LHS of BHXBs**
2. **HFQPO in SPL State of BHXBs**
3. **The Second Parameter in State Transition of BHXBs**
4. **The Origin of magnetic field in BHXBs**

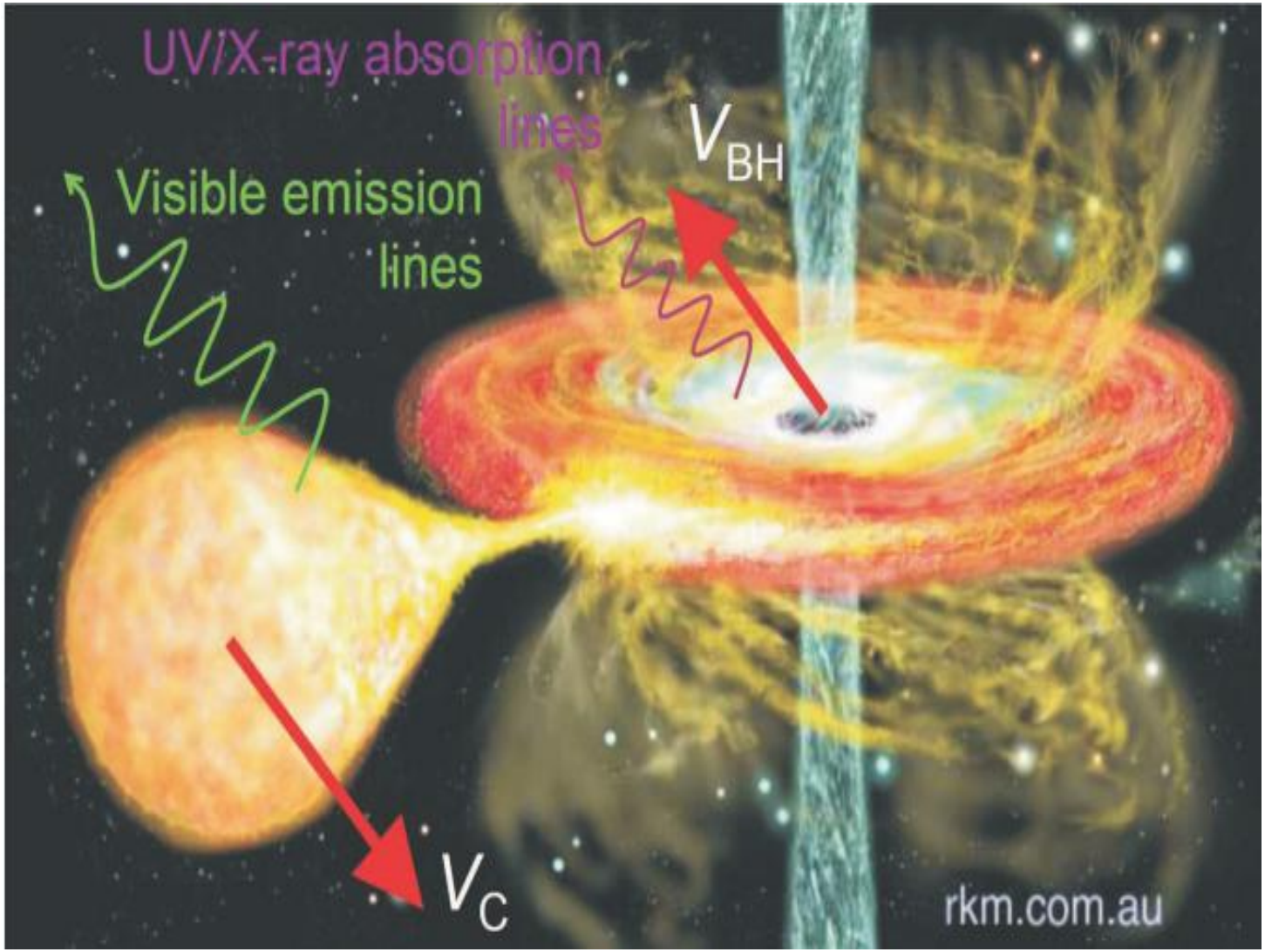

FIG. 1 A schematic drawing of outburst of BHXBs.

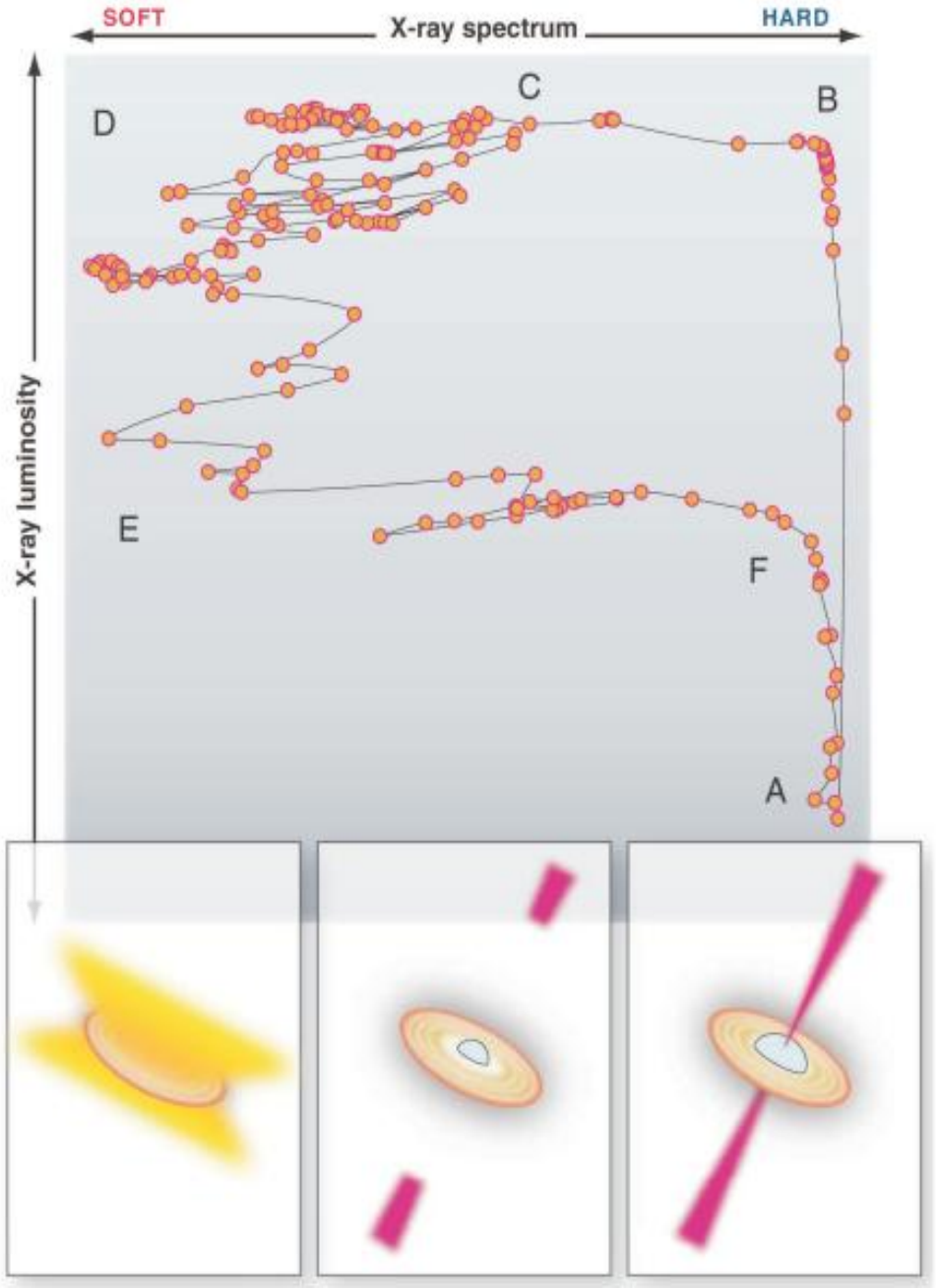

FIG. 2 A typical Hardness-Intensity-Diagram (HID) of spectral evolution of a BHXB, following A→B→C→D→E →F cycle (top). Steady or transient jets are present during the A→B or B→C→D stage. No jets are observed, but hot disk winds are ubiquitous during the D→E stage.

1. Jet production in LHS of BHXBs

1.1 Two promising mechanisms of powering jets

***Blandford-Payne (BP)* process,**

Jet is driven from accretion disk via large scale MF on the accretion disk

***Blandford-Znajek (BZ)* process,**

Jet is driven from a spinning black hole via large scale MF on the BH horizon

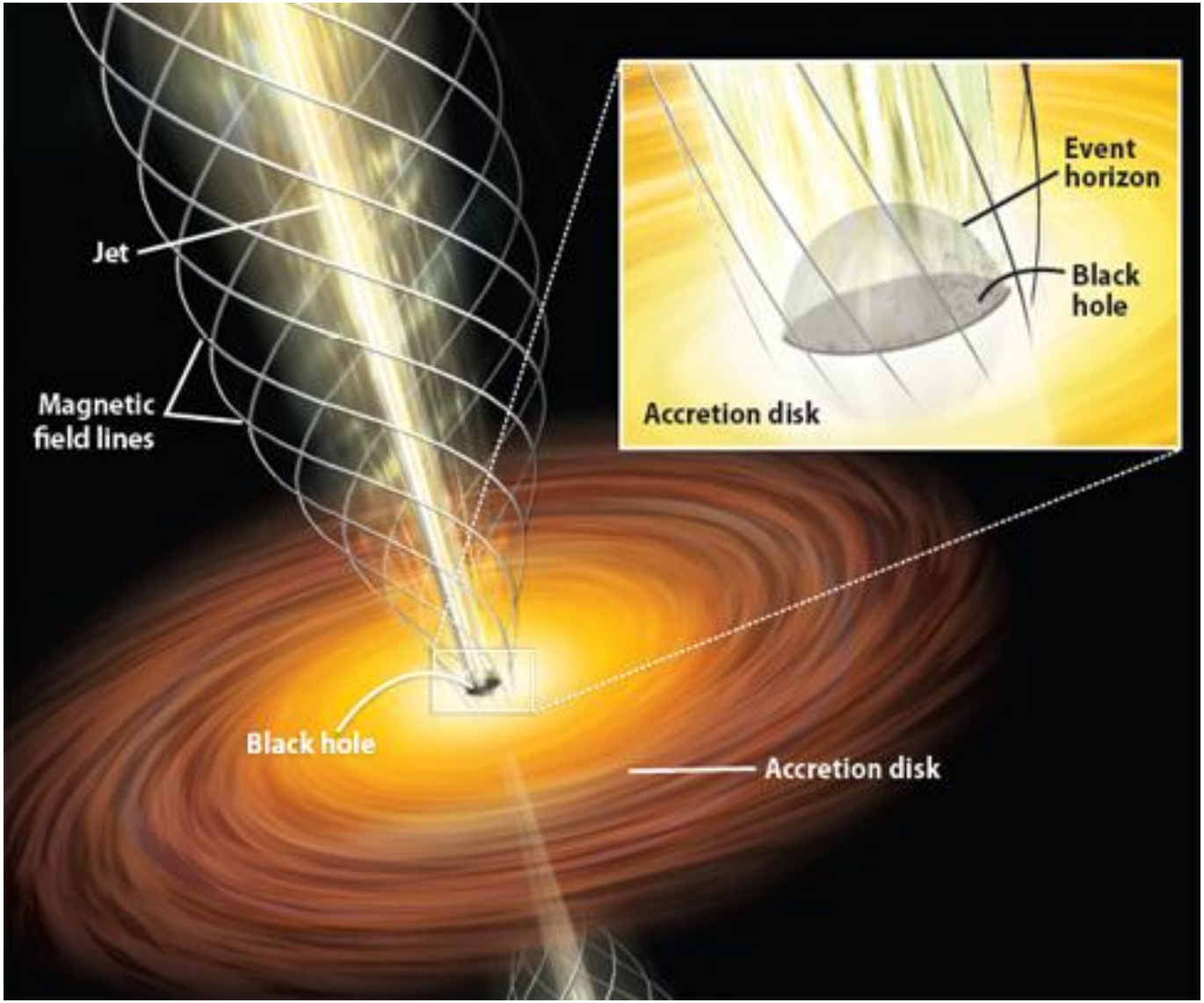

Fig. 3 The important role of magnetic field in jet production and collimation

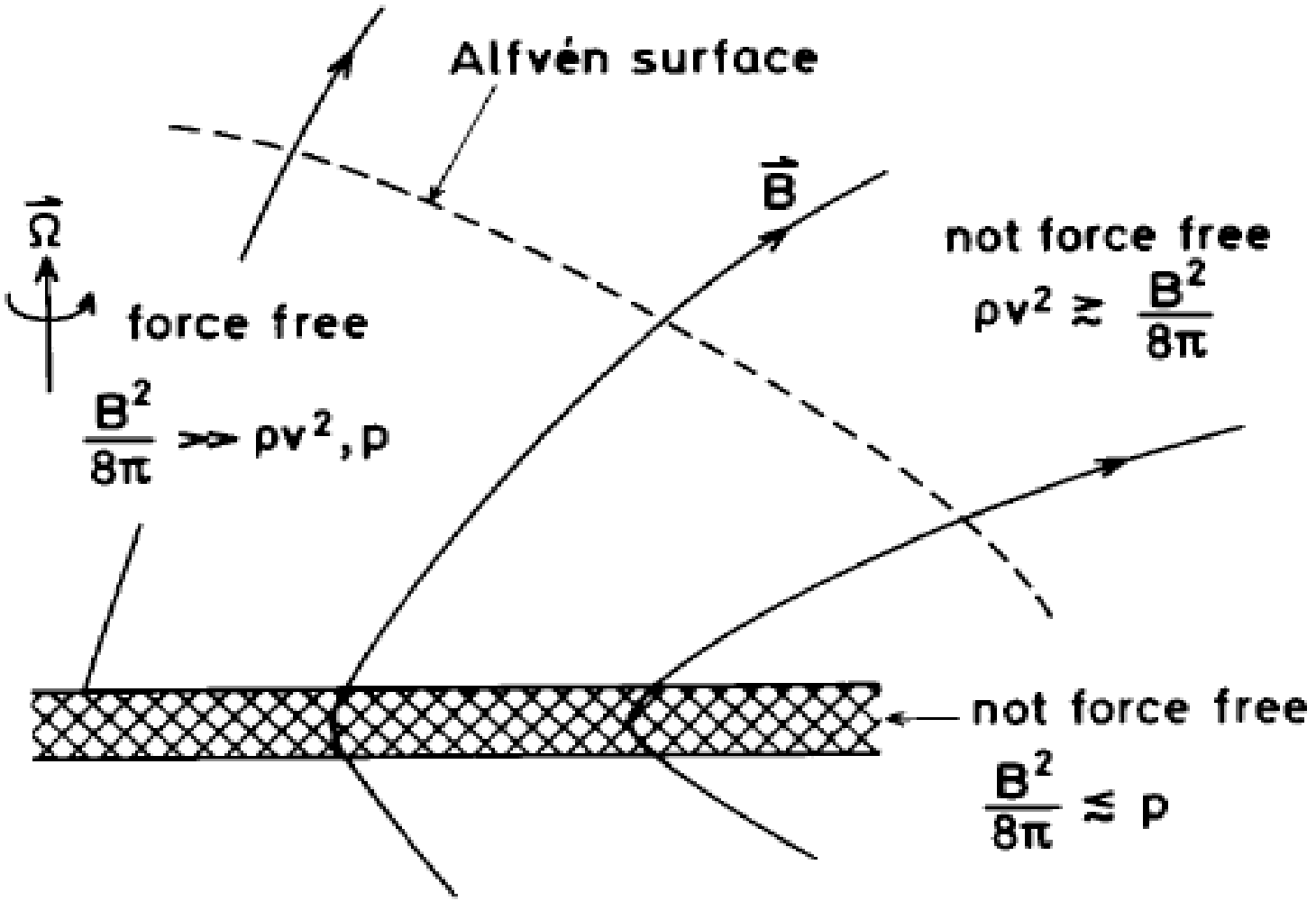

Fig. 4 The MF configuration for the BP process. Regions of force-free and non-force free magnetic field in a disk-driven wind.

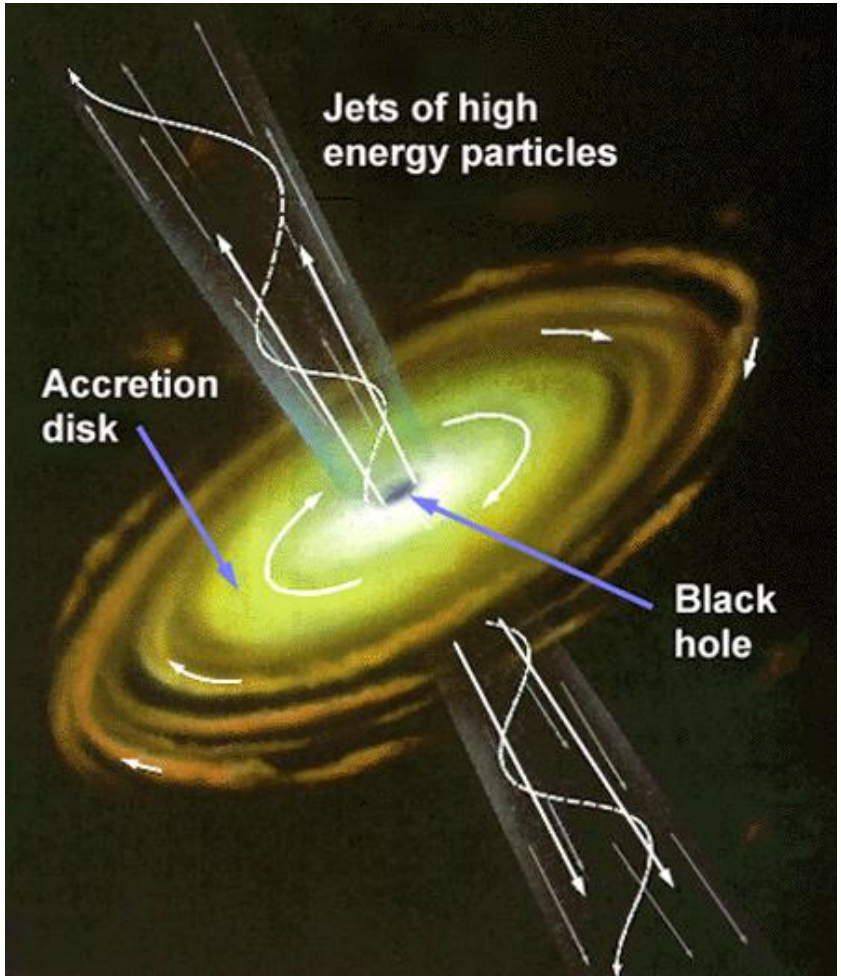

Fig. 5 The MF configuration for the BZ process: a spinning BH with a large-scale magnetic field may produce jet.

MF is transported from companion into accretion disk during the outburst of BHXBs

The coexistence of the BZ and BP processes

The large-scale magnetic field above the disk is related to the tangled small-scale magnetic field in the disk by (Livio et al 1999): $B_P \sim (H/R) B_D$

Inner ADAF + truncated thin disk model for Jet production in LHS

1.2 A Model for LHS of BHXBs

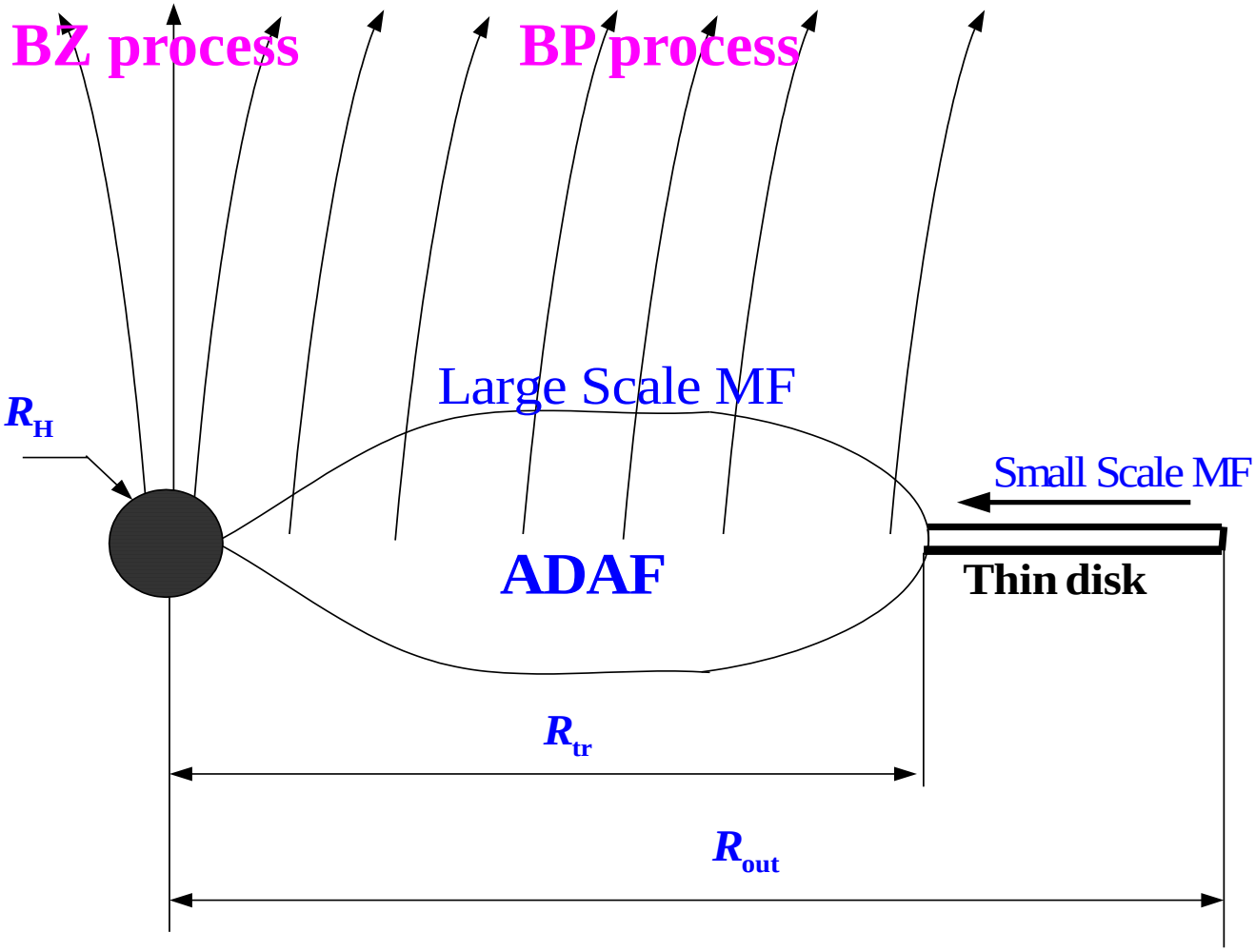

FIG. 6. Magnetic field transported in a truncated accretion disk from a companion

Magnetic flux carried by the accreting plasma is related to accretion rate M^dot,

$$\Phi(t) = \int_{t_b}^{t} \dot{\Phi} dt = 8.9 \times (\beta/\delta)^{1/2} \dot{M}_{Edd}^{1/2} \int_{t_b}^{t} \lambda_m^{1/2} (\dot{m}c)^{1/2} c dt$$

$\lambda_m \equiv B^2 / (8\pi\rho c^2)$ **Ratio of the magnetic energy density to the mass energy density**

$\beta = \upsilon_{tr} / c$ **Ratio of the radial velocity to speed of light**

$\delta = H_{tr} / R_{tr}$ **Ratio of the half height to the disk radius**

Both accretion rate m^dot and B_H vary with time:

$$\dot{m} = \dot{m}_0 \left(t/\tau\right)^{\alpha_m}, \qquad B_H = B_0 \left(t/\tau\right)^{\alpha_B}$$

The parameter τ is duration between t_b and time t_{IMS} reaching the intermediate state (IMS), and τ varies from several weeks to several months for different BHXBs in different outbursts,

$$0 \le t/\tau \le 1$$

The truncated radius can be determined by

$$R_{tr}^2 = 100\sqrt{2}\delta^{-1/2}\beta^{1/2}c^{3/2}\dot{M}_{Edd}^{1/2}\tau\frac{\lambda_m^{1/2}\left(t/\tau\right)^{\alpha_{tr}}}{B_0\left[\left(\alpha_m/2\right)+1\right]} - 99R_H^2,$$

where the parameter α_{tr} is crucial to the variation of R_{tr}.

$\alpha_{tr} = \left(\alpha_m/2\right) - \alpha_B + 1$ is positive or negative is a key for the variation of R_{tr}.

1.3 Fitting Results of LHS

Spectra of LHS of H1743-322 and GX 339-4 as shown in Figs. 7 and 8 with the input parameters in Tables 1 and 2, respectively.

Table 1. The parameters for fitting spectra of LHS of H1743-322 in four different dates

Date	t/τ	$\dot{m}$	r_{tr}	α_m	α_B	β_{gas}
1	0.01	0.005	132.09	0.5	1.3	0.93
2	0.13	0.018	123.89	0.5	1.3	0.90
3	0.29	0.027	121.43	0.5	1.3	0.85
4	0.45	0.034	120.10	0.5	1.3	0.80

Note: Date 1, 2, 3 and 4 in Table 1 indicate March 26, March 29, April 2 and April 6 in 2003, respectively.

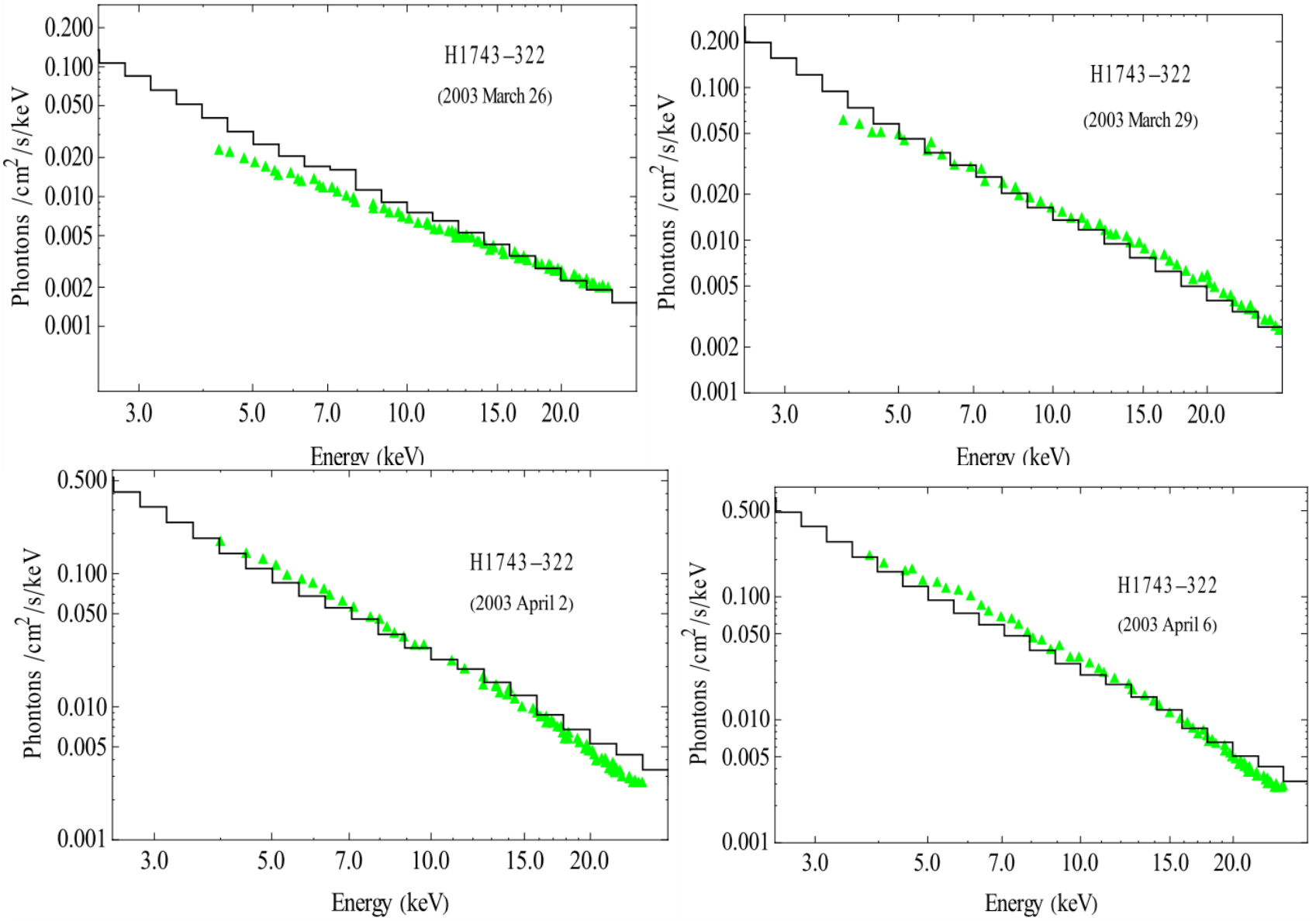

Fig. 7. The fitting spectra of LHS of H1743-322 with the jagged lines for the green triangles based on the four different dates.

Table 2. The parameters for fitting spectra of LHS of GX 339-4 in four different dates

Date	t/τ	$\dot{m}$	r_{tr}	α_m	α_B	β_{gas}
1	0.01	0.005	266.86	0.5	1.3	0.94
2	0.12	0.017	250.84	0.5	1.3	0.92
3	0.24	0.024	246.56	0.5	1.3	0.88
4	0.59	0.038	241.00	0.5	1.3	0.85

Note: Date 1, 2, 3 and 4 in Table 2 indicate Jan. 21, Feb. 2, Feb. 15 and March 26 in 2010, respectively. The dimensionless truncated disc radius is defined as $r_{tr} \equiv R_{tr}/R_H$.

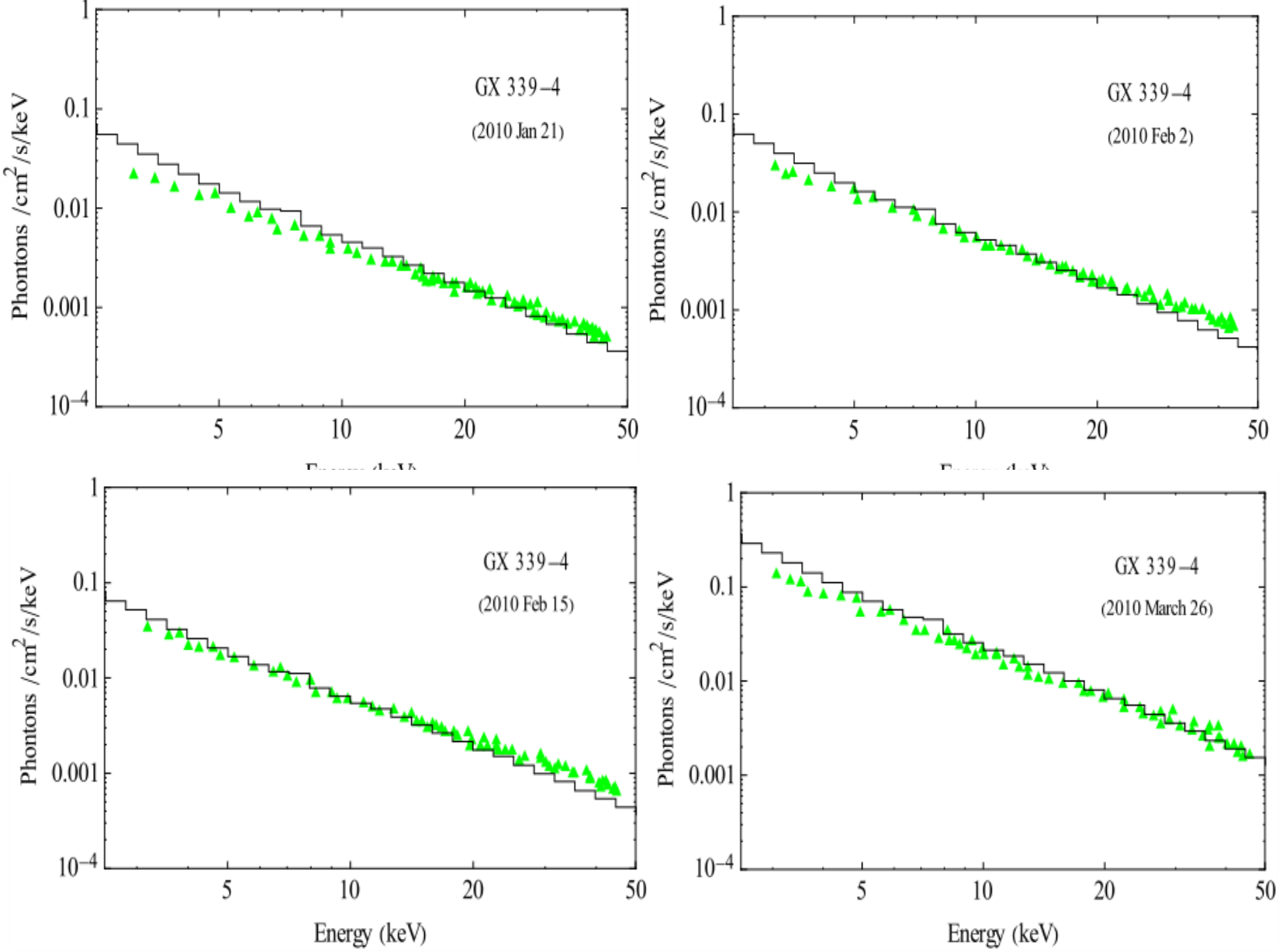

Fig. 8. The fitting spectra of LHS of GX 339-4 with the jagged lines for the green triangles based on the four different dates

$$L_X = L_X^I + L_X^{II},$$

where L_X^{II} is contributed by accretion flow, and

L_X^I is related to the BZ and BP powers as follows.

$$L_X^I = \eta_i \left(P_{BZ} + P_{BP} \right), \quad L_R = (1-\eta_i)\left(P_{BZ} + P_{BP} \right),$$

Table 3. The parameters for fitting the correlation between L_R and L_X for H1743-322 and GX 339-4 based on four different observations

Source	Spin	f_0	B_0	η_1	η_2	η_3	η_4
H1743-322	0.2	0.33	5.0×10^8	0.01	0.996	0.999	0.9994
GX 339-4	0.5	0.33	5.0×10^8	0.01	0.997	0.9987	0.9993

Note: The spin $a_* = 0.2$ for H1743-322 is taken from Narayan et al. (2012), while $a_* = 0.5$ for GX 339-4 is roughly estimated due to lack of data.

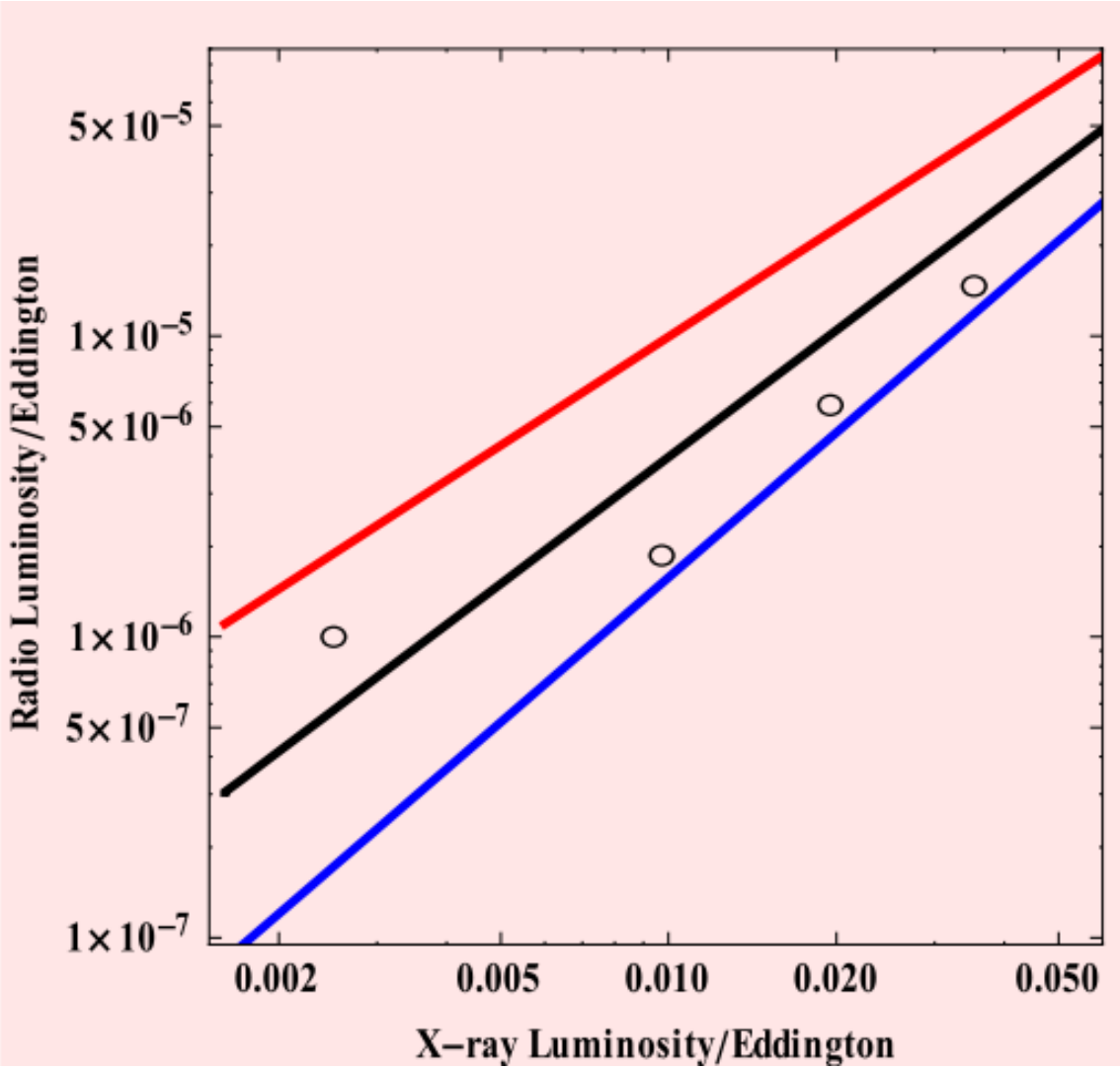

Fig. 9 The radio–X-ray correlations of H 1743−322 are plotted by combining the observation date with our model. the red, black and blue lines correspond to $L_R = 0.001 L_X^{1.2}$, $L_R = 0.001 L_X^{1.4}$ **and** $L_R = 0.001 L_X^{1.6}$, **respectively.**

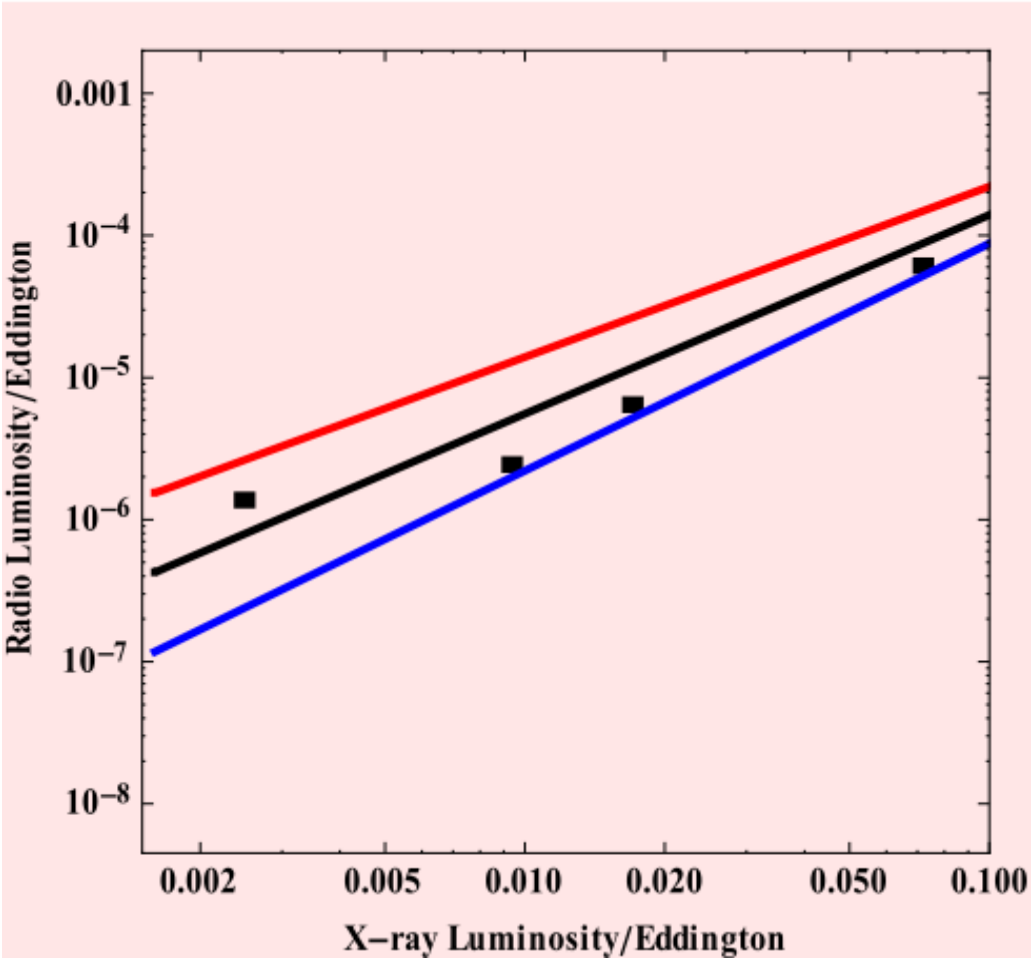

Fig. 10. The radio–X-ray correlations of GX 339−4 are plotted by combining the observation date with our model. The red, black and blue lines correspond to $L_R = 0.002 L_X^{1.2}$, $L_R = 0.002 L_X^{1.4}$ **and** $L_R = 0.002 L_X^{1.6}$, **respectively.**

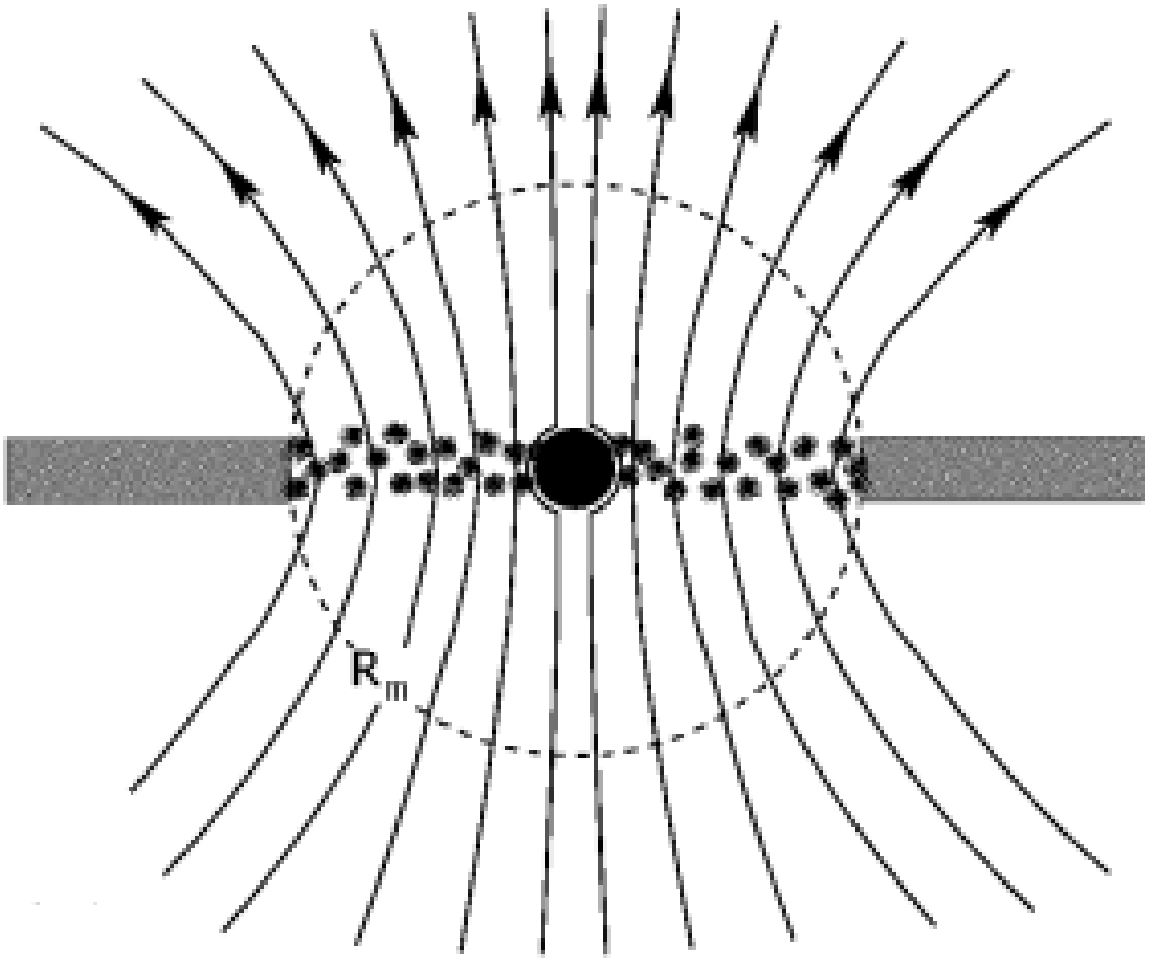

Fig. 11. MF configuration of MAD for transient episodic jets in IMS.

2. HFQPO in SPL State of BHXBs

The high-frequency quasi-periodic oscillations (HFQPOs) with 3:2 pairs have been observed in several X-ray binaries.

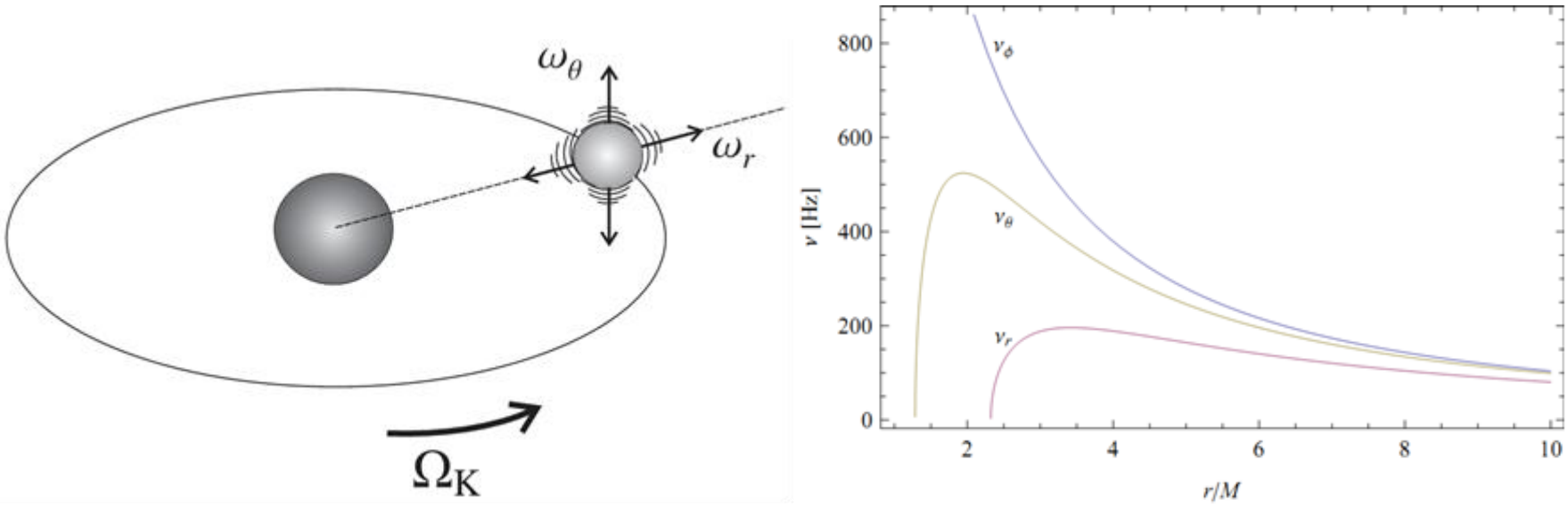

Fig. 12. A resonance model to interpret the HFQPO pairs Abramowicz & Kluzniak (2001)

Two uncertainties in resonance model (MacLintock & Remillard 2006).

(1) Whether epicyclic resonance could overcome the severe damping forces?

(2) Why the QPOs are associated with the SPL state of BH binaries?

These problems can be overcome by invoking the MC process with disk corona model (Gan et al. 2009; Huang et al. 2010)

Magnetic Coupling (MC) process is regarded as a variant of BZ process, connecting a spinning BH to the inner disk (van Putten 1999; Blandford 1999; Li 2000).

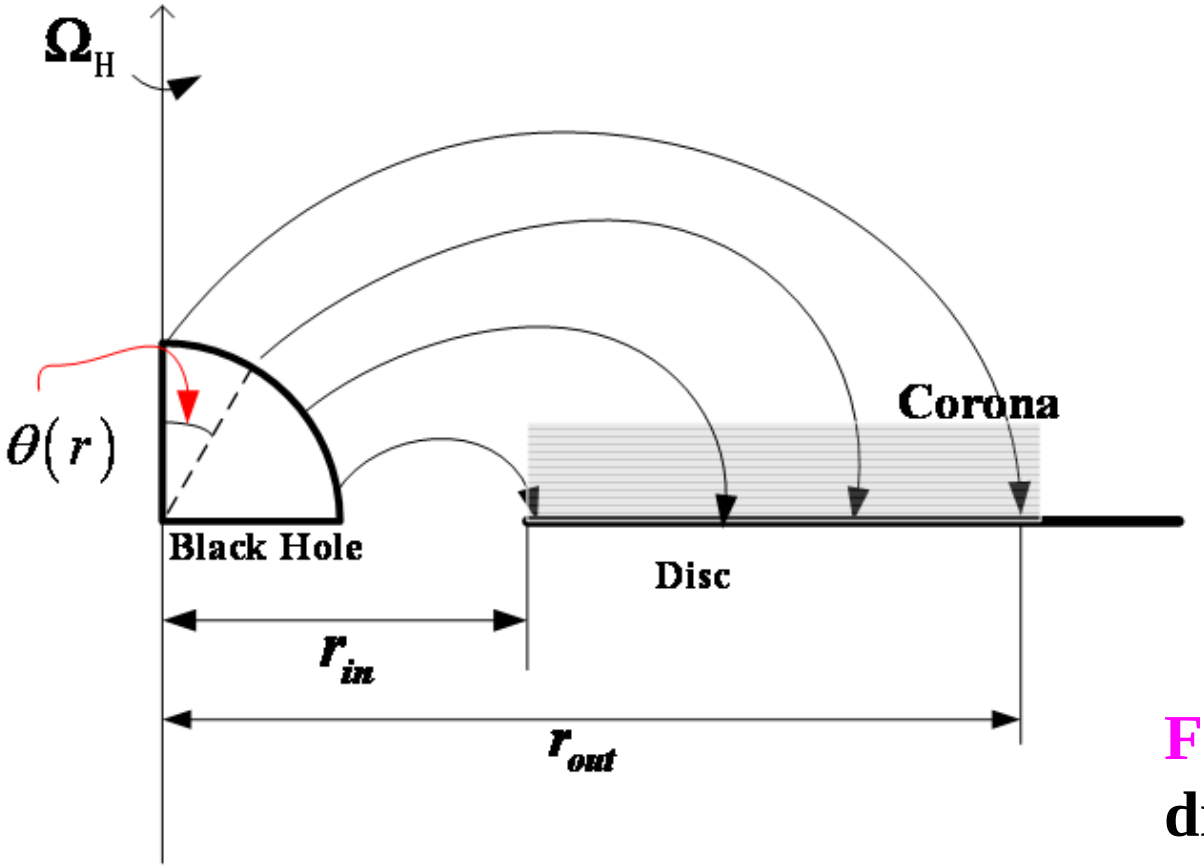

Fig. 13. A schematic drawing of disk-corona model

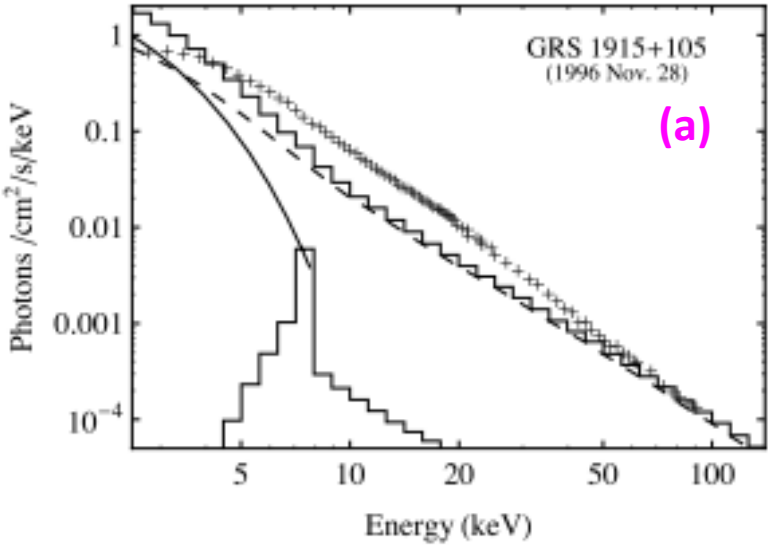

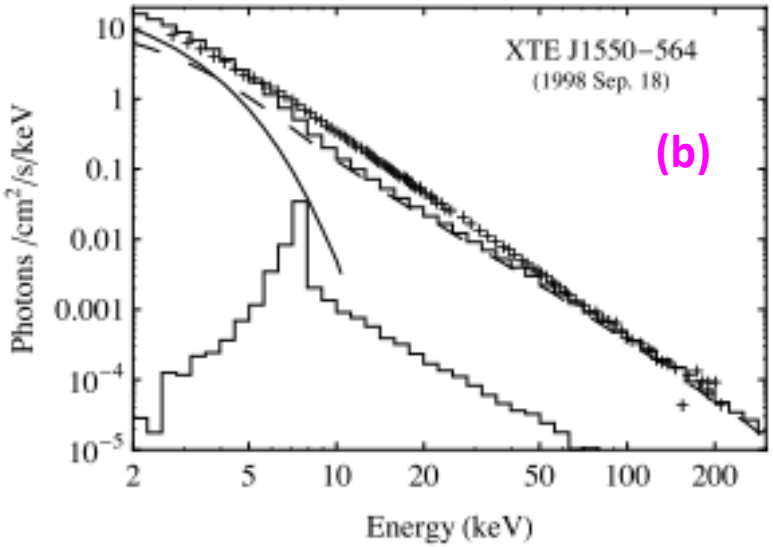

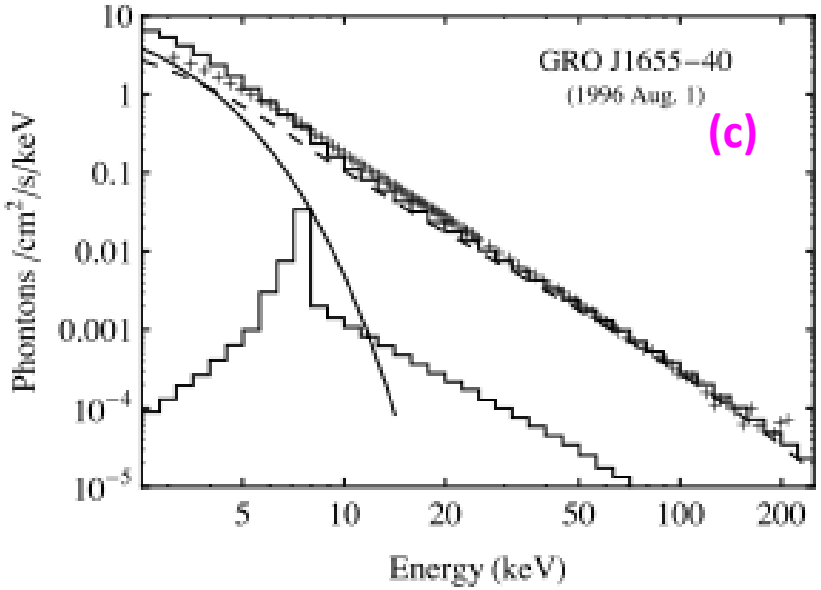

Fig. 14. Emerged spectra of the three sources in the SPL state: (a) GRS 1915+105 (1996 Nov. 28); (b) XTE J1550−564 (1998 Sep. 18) and (c) GRO J1655−40 (1996 Aug. 1).

3. The Second Parameter in State Transition of BHXBs

Accretion is the main source of energy in the outbursts of BHXBs, spending most of their time outside of outbursts at 'quiescence' with very low luminosities of $\sim 10^{30-32}$ erg s^{-1}.

3. The Second Parameter in State Transition of BHXBs

Accretion rate is the first parameter in state transition of BHXBs. However, the presence/absence of jets (disk wind), QPO, and hysteresis of state transitions cannot be interpreted by only accretion rate.

MF can be regarded as the second parameter in state transition of BHXBs (Spruit & Uzdensky 2005; Meyer-Hofmeister, Liu & Meyer 2005; King et al. 2012).

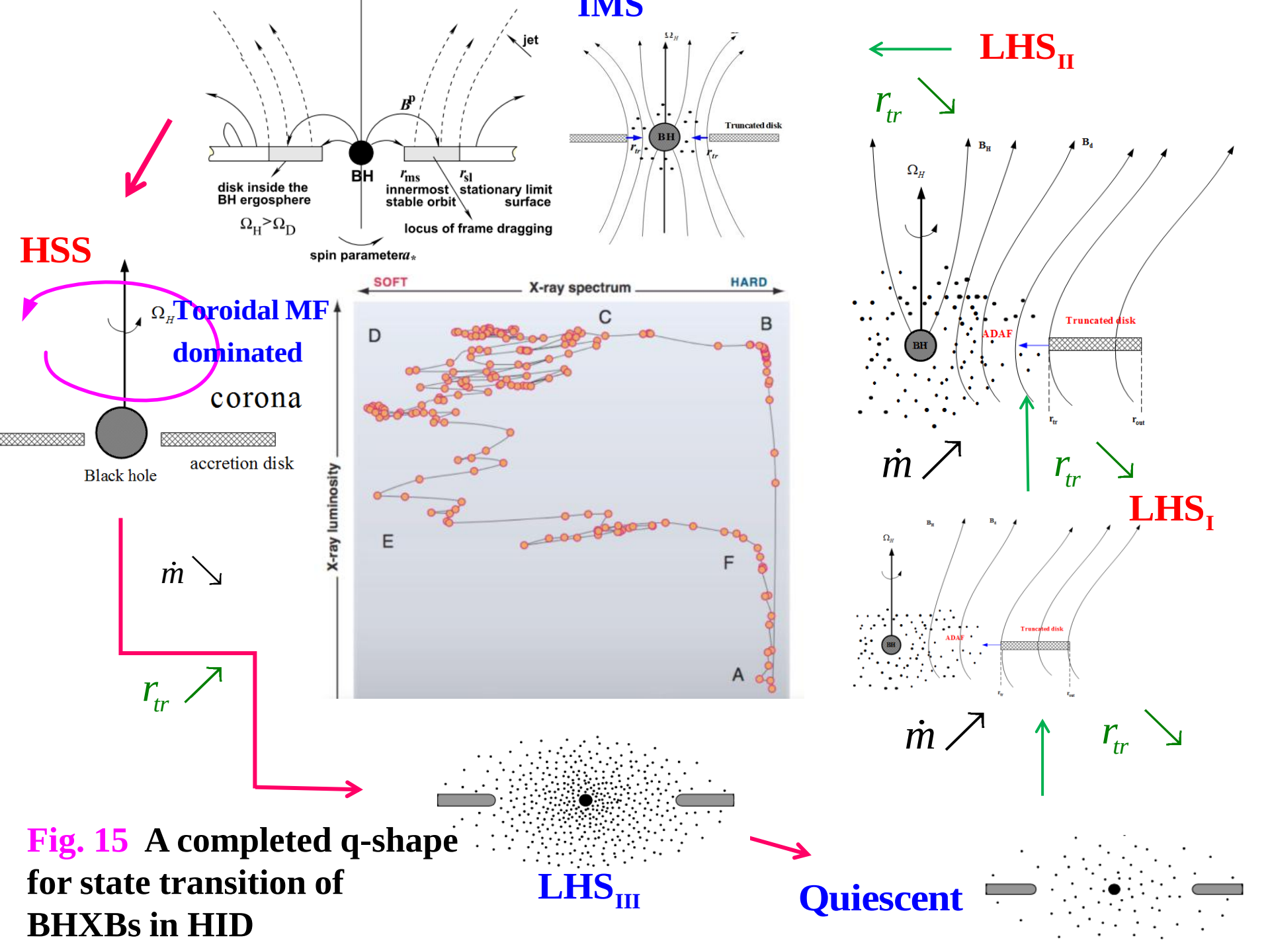

Fig. 15 **A completed q-shape for state transition of BHXBs in HID**

4. The Origin of magnetic field in BHXBs

THREE POSSIBILITIES:

(i) Seed magnetic field from the companion;

(ii) 'Dynamo mechanism' due to differential rotation of accretion disk.

(iii) Toroidal current flowing in disk

Zhao et al. (2009) obtained four types of configuration of the magnetic connection (MC) based on the following toroidal electric current, arising probably from deviation from electric neutrality of accreting plasma.

$$j = j_0 \left(r / r_{ms} \right)^{-n} \delta\left(cos\theta \right), \qquad r_{ms} \le r \le \lambda_d r_{ms}$$

where *n* and λ_d can be adjusted for different MF configurations.

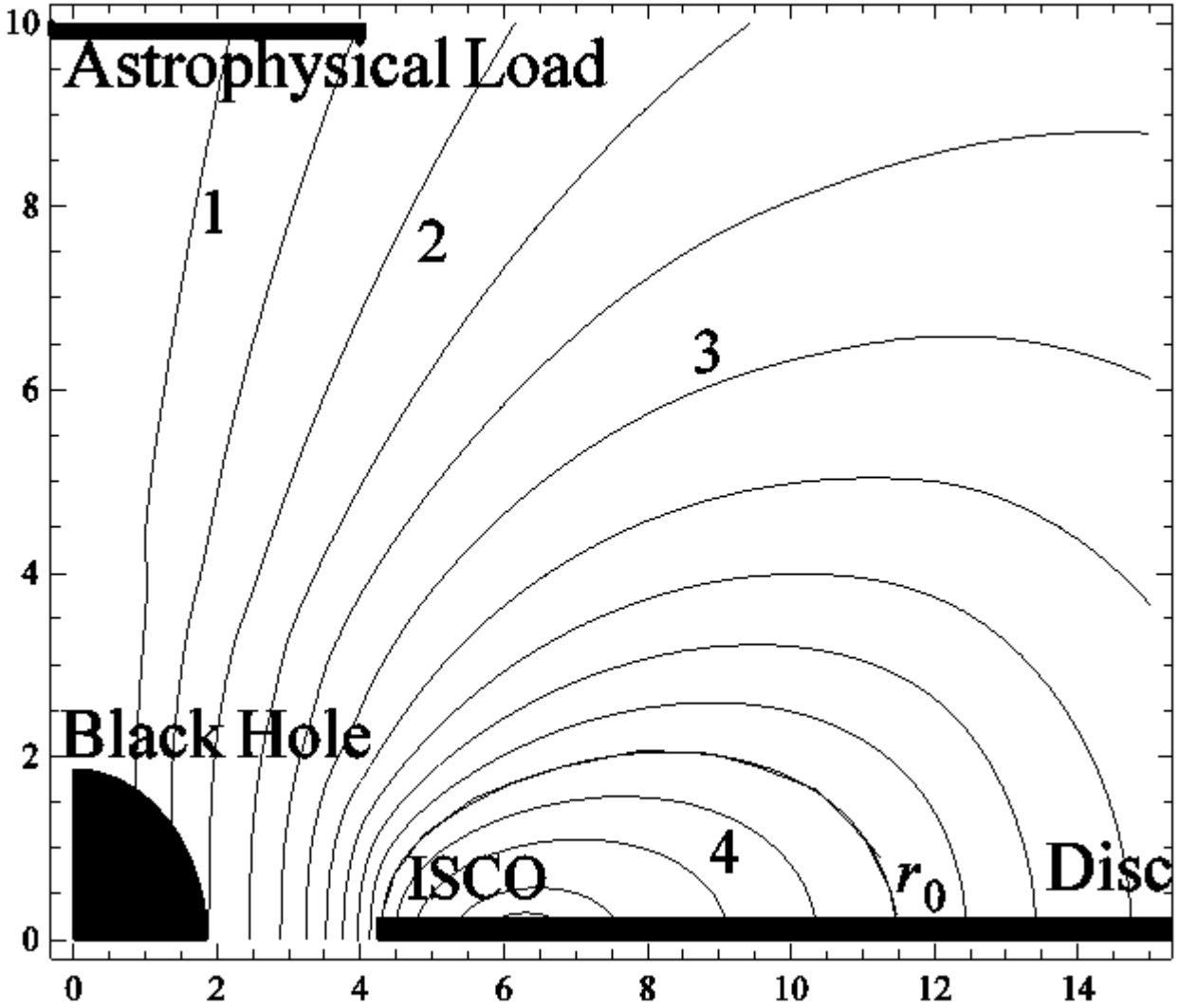

Fig. 16. The magnetic field configuration generated by toroidal electric current distributed continuously over the inner region of a thin disc around a Kerr BH with $a_* = 0.5,\ n = 3.0,\ \lambda_d = 3$

Similar magnetic field configurations have been discussed by some authors.

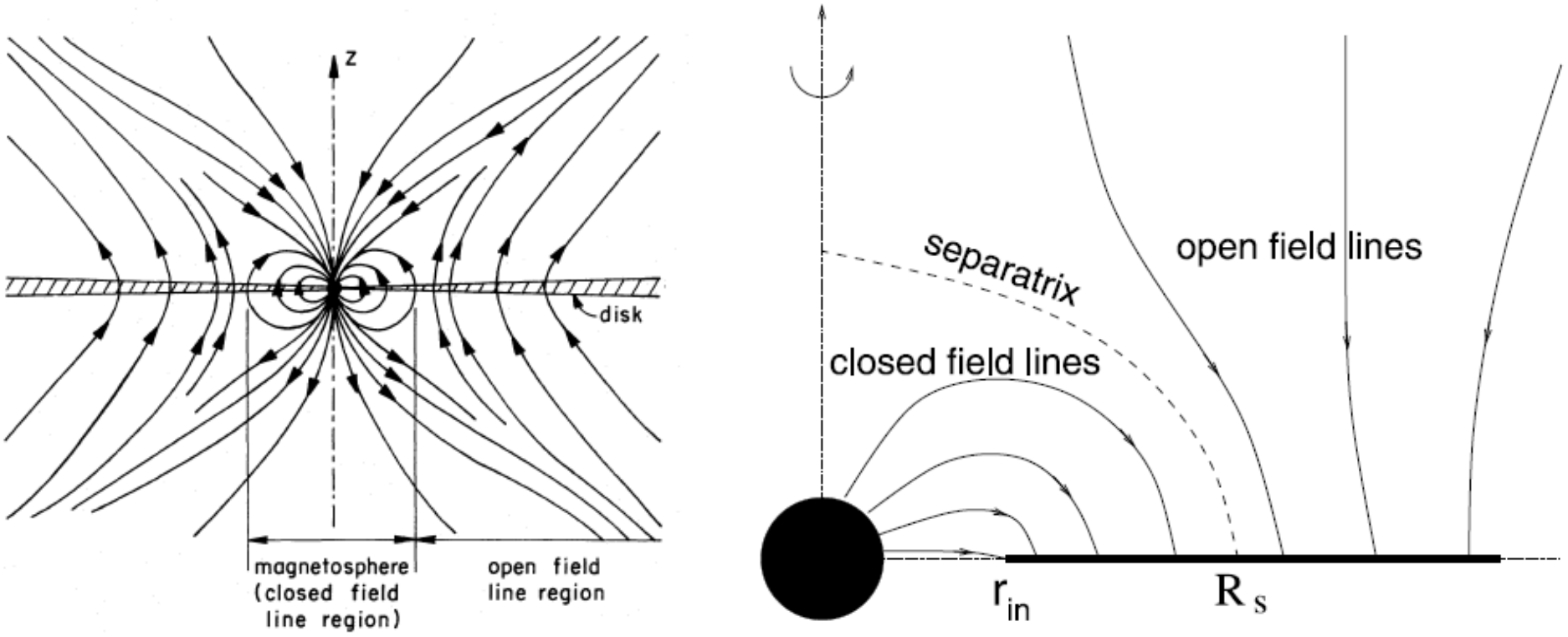

Fig. 17. The magnetic field configurations with open and closed field lines anchored at BH accretion disk. Left and right panels are adopted from Lovelace (1995) and Uzdensky (2005), respectively.

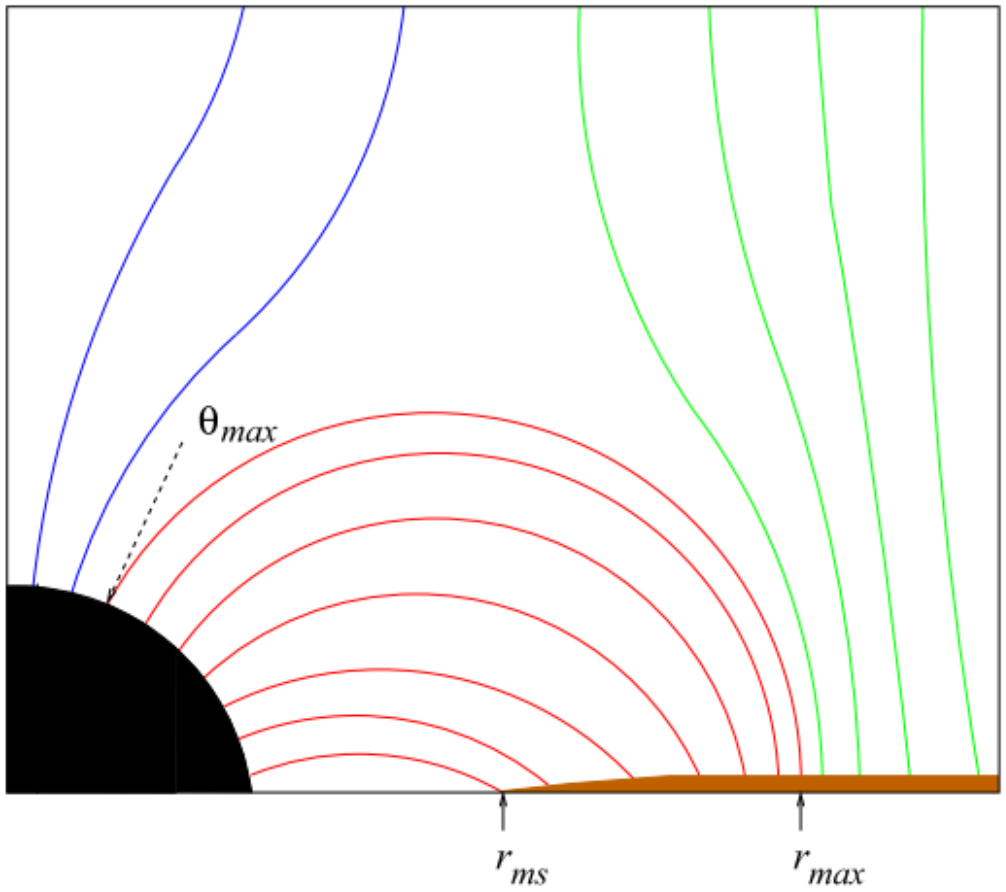

Fig. 18. **The magnetic field configurations with open and closed field lines anchored at BH accretion disk adapted from Kovacs et al. (2011)**

Thanks